And in the Darkness Bind Them: Equatorial Rings, B[e] Supergiants, and the Waists of Bipolar Nebulae[1]

Nathan Smith[2,3,4,5], John Bally[3,5], and Josh Walawender[3,5,6]

ABSTRACT

We report the discovery of two new circumstellar ring nebulae in the western Carina Nebula, and we discuss their significance in stellar evolution. The brighter of the two new objects, SBW1, resembles a lidless staring eye and encircles a B1.5 Iab supergiant. Although seen in Carina, its luminosity class and radial velocity imply a larger distance of ∼7 kpc in the far Carina arm. At that distance its size and shape are nearly identical to the equatorial ring around SN1987A, but SBW1's low N abundance indicates that the ring was excreted without its star passing through a red supergiant phase. The fainter object, SBW2, is a more distorted ring, is N-rich, and is peculiar in that its central star seems to be invisible. We discuss the implications of these two new nebulae in context with other circumstellar rings such as those around SN1987A, Sher 25, HD 168625, RY Scuti, WeBo1, SuWt2, and others. The ring bearers fall into two groups: Five rings surround hot supergiants, and it is striking that all except for the one known binary are carbon copies of the ring around SN1987A. We propose a link between these B supergiant rings and B[e] supergiants, where the large spatially-resolved rings derive from the same material that would have given rise to emission lines during the earlier B[e] phase, when it was much closer to the star. The remaining four rings surround evolved intermediate-mass stars; all members of this ring fellowship are close binaries, hinting that binary interactions govern the forging of such rings. Two-thirds of our sample are found in or near giant H II regions. We estimate that there may be several thousand more dark rings in the Galaxy, but we are scarcely aware of their existence – either because they are only illuminated in precious few circumstances or because of selection effects. For intermediate-mass stars, these rings might be the pre-existing equatorial density enhancements invoked to bind the waists of bipolar nebulae.

Subject headings: circumstellar matter — H II regions — stars: mass-loss — stars: winds, outflows

1. INTRODUCTION

Non-spherical mass loss is a key ingredient for understanding the roles of rotation, magnetic fields, and close binary interactions in various stages of stellar evolution. Bipolar structure is common in nebulae

[1]Based in part on observations made at the Clay Telescope of the Magellan Observatory, a joint facility of the Carnegie Observatories, Harvard University, the Massachusetts Institute of Technology, the University of Arizona, and the University of Michigan.

[2]Astronomy Department, University of California, 601 Campbell Hall, Berkeley, CA 94720; nathans@astro.berkeley.edu

[3]Center for Astrophysics and Space Astronomy, University of Colorado, 389 UCB, Boulder, CO 80309

[4]Visiting Astronomer at the New Technology Telescope of the European Southern Observatory, La Silla, Chile.

[5]Visiting Astronomer, Cerro Tololo Inter-American Observatory, National Optical Astronomy Observatory, operated by the Association of Universities for Research in Astronomy, Inc., under cooperative agreement with the National Science Foundation.

[6]Institute for Astronomy, 640 North A'ohoku Place, Hilo, HI 96720-2700

surrounding evolved stars across the HR Diagram, most notably in planetary nebulae (Balick & Frank 2002) and in more massive hot stars like luminous blue variables (LBVs). Many bipolar nebulae have a dense torus or ring at their pinched waist where the polar lobes meet at the equator, as seen in prototypical objects like η Carinae (Smith et al. 2002*a*) and in dramatic *Hubble Space Telescope* (*HST*) images of planetary nebulae like MyCn 18 (Sahai et al. 1999), NGC2346,[1] and NGC7027 (Latter et al. 2000).

Perhaps the most outstanding and familiar example of such equatorial structure is the inner ring around SN1987A (Plait et al. 1995; Burrows et al. 1995; Crotts & Heathcote 1991; Crotts et al. 1989). In SN1987A as well as planetary nebulae, the prevailing interpretation for the formation of these equatorial rings and bipolar nebulae has been that a fast low-density wind expands into an asymmetric slow dense wind from a previous red giant or supergiant phase (e.g., Blondin & Lundqvist 1993; Martin & Arnett 1995; Collins et al. 1999; Frank & Mellema 1994; Frank 1999). This requires that the slow wind had a strong equatorial density enhancement (i.e. a disk) that can be swept-up to form a ring, but the origin of this putative pre-existing disk is unclear, and evidence of them around red supergiants is non-existent.

The formation of equatorial disks by single stars has been of continued interest to the Be star community, since these stars are rapid rotators. B[e] supergiants are suspected to be their high luminosity analogs (e.g., Zickgraf et al. 1986). The wind-compressed disk model (Bjorkman & Cassinelli 1993) suggests that rapidly rotating stars will form disks as material ejected at mid-latitudes is directed toward the equator. While such disks are inhibited in hot stars with line-driven winds because of the effects of gravity darkening and velocity-dependent forces (Owocki et al. 1996; Cranmer & Owocki 1995), wind compression may still operate in other circumstances. Ignace et al. (1996) suggested that cool stars may experience moderate compression, while Smith & Townsend (2007) propose that thin disks can form in continuum-driven LBV eruptions. Changes in ionization with latitude on a gravity-darkened rotating star has been suggested to play a role in disk formation as well (e.g., Lamers & Pauldrach 1991; Cure et al. 2005). However, any disk formation around cool stars requires rapid rotation much in excess of rotation rates expected for the distended envelopes of red giants and supergiants. Indeed, Collins et al. (1999) estimated that while in the red supergiant phase, the progenitor of SN1987A must have been rotating at $\gtrsim$0.3 of its critical breakup speed to produce the observed nebular morphology — which is impossible for normal single-star evolution — so they conclude that the red supergiant was most likely spun-up by swallowing a companion. Thus, close binary interactions and mergers are often taken as potential sources of angular momentum to focus material toward the equator. Magnetic fields may provide yet another avenue for the formation of equatorial disks or rings (ud-Doula & Owocki 2002; Washimi et al. 1996; Townsend & Owocki 2005; Matt & Balick 2004).

The equatorial ring around SN1987A is quite unusual in that it really is a hollow ring and not just a limb-brightened shell or pinched waist of an hourglass.[2] A virtual twin of SN1987A's equatorial ring has been discovered in the Milky Way: the ring around the blue supergiant Sher 25 in NGC 3603 (Brandner et al. 1997). More recently, Smith (2007) has suggested another twin of SN1987A's nebula around the Galactic LBV candidate HD168625. Two other notable examples are the ringed planetary nebulae WeBo1 (Bond et al. 2003) and SuWt2 (Schuster & West 1976). Regardless of the nature of their central stars, these objects are similar in the unusually distinct ring morphology of their ejecta. To this class we add two more examples, both discovered in the Carina Nebula (NGC 3372; see Fig. 1).

[1]See the Hubble Heritage image at `http://heritage.stsci.edu/1999/37/index.html`.

[2]Here we are using the word "ring" to denote a thin toroid in 3-dimensional space, like a wedding ring, as distinguished from an apparent ring on the sky caused by a limb-brightened spherical shell like the "ring nebulae" around Wolf-Rayet stars, for example.

2. OBSERVATIONS

2.1. CTIO Mosaic Images

The discovery of the two ring nebulae described in this paper was made serendipitously during a narrowband imaging survey of the Carina Nebula, although these images are not shown here as they are of lesser quality than the Magellan images described below. We surveyed the entire $2\overset{\circ}{.}5\times4^\circ$ area of the giant Carina Nebula on 2003 March 10 using several pointings with the 8192×8192 pixel imager MOSAIC2 mounted at the prime focus of the CTIO 4m Blanco telescope. This camera has a large $35\overset{\prime}{.}4$ field of view, which allowed us to efficiently survey the whole nebula using the [O III] λ5007, Hα+[N II], and [S II] $\lambda\lambda$6717,6731 narrowband filters, plus the i' broadband filter. Further details of the observations and data reduction can be found in previous papers from the same project (e.g., Smith et al. 2004, 2005*a*). Because we were trying to maximize efficient spatial coverage of the nebula in multiple filters, we did not do a full set of MOSDITHER exposures to correct for the $\sim3''$ interchip gaps. One of the objects of interest here (SBW2) ended up straddling a gap, motivating the subsequent imaging with the 6.5m Magellan telescope described below. Both nebulae were easily recognized as circumstellar rings in the Hα+[N II] filter images, but no circumstellar emission was seen in images in the other filters taken with similar 5–10 minute exposure times.

The positions of these two ring nebulae are listed in Table 1, and their approximate locations are marked on the wide-field image in Figure 1. These absolute sky coordinates from the MOSAIC2 images were determined with reference to USNO catalog stars.

2.2. Magellan Images

Following the initial discovery in CTIO images, we obtained narrowband Hα images of the two Carina ring nebulae on 2005 February 21 using the CCD imager MagIC mounted on the 6.5m Clay telescope of the Magellan Observatory. MagIC[3] has a 2048×2048 pixel SITe detector, with a spatial pixel scale of $0\overset{\prime\prime}{.}069$ and a $142''\times142''$ field of view on the 6.5m Clay telescope. The night was decidedly non-photometric with patchy and highly-variable cirrus, but the seeing was still quite good at $\sim0\overset{\prime\prime}{.}6$. SBW1 was bright enough to observe easily with a 6.5m telescope looking through clouds, and we took a set of 3 exposures of 120 sec each. SBW2 is much fainter and while we observed it the cloud cover became more crippling, but with periodic thin patches. Therefore, we took a long series of about 30 consecutive 300 s exposures as the clouds rolled by, and we selected only the highest-quality images (the ones with the largest number of counts and best seeing) to shift and add together. The small $0\overset{\prime\prime}{.}069$ pixels were rebinned by a factor of 3 to larger pixels of $0\overset{\prime\prime}{.}207$. The final H$\alpha$+[N II] images of the two rings are shown in Figure 2, while intensity tracings through the middle of each ring are shown in Figure 3.

2.3. NTT/EMMI Echelle Spectra

We used the ESO Multi-Mode Instrument (EMMI) on the NTT to obtain high resolution spectra of SBW1 and SBW2 on the nights of 2003 March 11 and 12, respectively (one and two nights after their discovery in CTIO images). For both targets we used the number 10 echelle grating and EMMI's red CCD

[3]see `http://www.ociw.edu/lco/magellan/instruments/MAGIC/`

with a 4096×4096 pixel MIT/LL detector, a pixel scale of 0.″166×0.058 Å, and R=$\lambda/\Delta\lambda$=28,000 (10 km s^{-1}) at wavelengths near Hα. We calibrated the wavelengths using an internal emission lamp.

For SBW1, we used EMMI in cross-dispersed mode, with a 15″×1″ slit aperture, oriented at P.A.=45° across the minor axis of the nebula (see Fig. 4*a*). SBW1 is in a region of bright nebular emission in the western Carina Nebula, so we also obtained similar exposures of an adjacent position offset by 30″ SE to subtract emission from the nebula and sky. The red [S II] $\lambda\lambda$6717,6731 doublet was faintly visible in the resulting spectra, but the signal to noise in the 30-minute exposure was too low to provide a meaninful measure of the electron density. This is consistent with the fact that we detected no extended structure in narrowband [S II] images. Aside from Hα and [N II], no other emission lines were detected in the nebula. The order including Hα+[N II] emission is shown in Figure 5*a*, while tracings of the spectrum through the NE and SW portions of the ring are shown in Figure 5*b*, and an extracted spectrum of the central star is shown in Figure 5*c*. Detailed views of the long-slit kinematics for Hα and [N II] λ6583 are shown in Figures 6*a* and *b*, respectively.

For SBW2, which has a larger size on the sky, we used a longer 6′×1″ aperture, with a flat mirror in the beam instead of a cross-disperser, and we used a narrowband order-sorting filter to isolate Hα+[N II]. This long slit was also oriented at P.A.=45° through the minor axis of the ellipse (Fig. 4*b*). Unfortunately, SBW2 was observed at the end of the night and had less than half much time as we would have liked, an the resulting signal to noise of the spectrum was much less than half of what this object deserved. The resulting spectrum is noisy and is not displayed here (dominated by read noise, since it is in a region of very faint nebular background emission; see Fig. 1). These spectra are useful, however, because although we detected the Hα+[N II] lines, we detected no Doppler shifts from one side of the ring to the next. The limiting resolution of 10 km s^{-1} for these data then imply a limiting intrinsic radial expansion speed of ±8 km s^{-1} (±16 km s^{-1} across the diameter of the ring) when corrected for the disk inclination angle (see below).

2.4. CTIO 4m/RC Spec Spectra

We used RC Spec on the CTIO 4m to obtain medium-resolution (R≈6,000) red spectra of SBW1, SBW2, and SuWt2 on 2006 March 15. RC Spec[4] is the cassegrain grating spectrograph on the V.M. Blanco 4m telescope, equipped with a Loral 1k×3k CCD detector. We used grating G380 and filter GG495 to sample wavelengths $\Delta\lambda$=5480–7153 Å, with a pixel scale of 0.″5×0.55 Å, and an effective 2-pixel spectral resolution of roughly 50 km s^{-1}. The slit width was set at 0.″8, matched approximately to the seeing, with the long slit oriented as in Figure 4 for SBW1 and SBW2, and along the major axis of the ring at P.A.=–45° for SuWt2. We used total integration times of 9 min for SBW1, and 40 min for SBW2 and SuWt2. The conditions were photometric, and the data were flux calibrated using observations of the spectrophotometric standards LTT3218 and LTT4816. Wavelength calibration was performed with reference to an internal HeNeAr lamp. Emission from the background sky and H II region was subtracted by sampling nebular emission along the slit adjacent to each object.

The extracted flux-calibrated spectra are shown in Figure 7, and line intensities for several emission lines relative to Hα=100 are listed in Table 2. The relative line intensities in Table 2 have been dereddened.

A reddening of $E(B-V)$=0.5 for SBW2 is a standard value for relatively unobscured regions in Carina

[4]see `http://www.ctio.edu/spectrographs/4m_R-C/4m_R-C.html`.

(e.g., Smith et al. 2005b), while we chose a higher value of $E(B-V)$=1.0 for SBW1, even though it too appears in Carina, for reasons justified later in §3.1.2. The value of $E(B-V)$=0.25 for SuWt2 was determined by matching the continuum shape of the central star in our spectra to an early A-type photosphere (however, this value is very uncertain due to the small overall wavelength range of our red spectra). Uncertainties are a few percent for the brightest lines, and several to 10% for the faintest lines. For SBW1 and SBW2 we give upper limits to the intensity of [N II] λ5755, since it is important for constraining the electron temperature and chemical abundances.

On 2006 March 16 we also obtained a blue spectrum of the central star of SBW1 with RC Spec on the CTIO 4m telescope in order to determine the spectral type of the central star. Two 150-second exposures covering roughly 3000–6000 Å were obtained with the 0.″67 slit along a position angle of about 10°. The data were reduced in the standard way, and emission from the sky and background H II region was subtracted by fitting background diffuse emission along the slit. Figure 8 shows a normalized spectrum extracted from a ∼1.″5 segment of the slit.

2.5. New observations of SuWt2 and WeBo1

Using the MOSAIC2 camera on the CTIO 4m telescope (during the same survey of star-forming regions when we discovered SBW1 and SBW2 as noted earlier in §2.1), we also obtained an Hα+[N II] image of another ring nebula called SuWt2 on the same night of 2003 March 10. SuWt2 was originally discovered on red photographic plates by Schuster & West (1976), but the new CCD image presented here (Fig. 9) has greater sensitivity and was obtained in better seeing conditions with a narrow filter. The new image of SuWt2 will be discussed in §5.

The ring nebula WeBo1 was first reported by Bond et al. (2003), who discussed its morphology in images and the properties of the central star. It was discovered independently on 1999 October 6 during our narrow-band imaging survey of nearby star-forming molecular clouds, seen on a wide-field narrow-band Hα image obtained with the 1° field-of-view MOSAIC CCD camera mounted on the Kitt Peak 0.9 meter telescope. This prompted us to obtain additional imaging and spectroscopy of WeBo1.

A deep Hα image was obtained at the f/10 Nasmyth focus of the Astrophysical Research Consortium (ARC) 3.5 meter telescope at the Apache Point Observatory near Sunspot, New Mexico, on 2001 September 25 using a 2048 × 2048 pixel CCD (SPICam) with a 40 Å passband Hα filter and a total exposure time of 1160 seconds. The CCD was binned 2×2 to provide a pixel scale of 0.″22. This image is shown in Figure 10*a*. Low dispersion (R = 500) spectra were then obtained on 2001 September 26 with the Dual-channel Imaging Spectrometer (DIS) at the 3.5 meter telescope, using a 0.″9 slit width. The slit was oriented along the major axis of the ring as indicated in Figure 10*a*, and included the light of the two brightest stars located in the ring interior. The resulting spectrum of the northern portion of the ring is shown in Figure 10*b*. Additionally, a high-resolution (R = 20,000) spectrum, shown in Figure 10*c*, was obtained on 2000 December 18 with the HIRES spectrometer on the Keck I telescope. The aperture traced the northern edge of the nebula with the slit aligned along the major axis of the ring.

Finally, we searched for J = 1–0 CO emission in a 10′ diameter box using the 16 beam SEQUOIA array at the 14 m diameter radio telescope at the Five College Radio Astronomy Observatory (FCRAO) near Amherst Massachusetts on 2001 January 6. No emission was found at any velocity above an rms brightness temperature level of 0.3 K in 92 kHz wide channels.

3. RESULTS

3.1. Imaging and Spectroscopy of SBW1

3.1.1. Basic Morphology and Kinematics

SBW1 appears as a distinct, almost perfectly smooth elliptical nebula with a well-defined outer edge in Figure 2*a*. With its bright central star it resembles a wide-open staring eye, lidless and wreathed in flame, probably deserving a nickname like the "Eye of Sauron" nebula; later in this paper we will discuss its relation to the other rings. This ring is brightest at its southeast and northwest apexes, due to limb-brightening, and the interior of the ring is partially filled-in with diffuse emission. Figure 3*a* shows an intensity tracing through the minor axis of the nebula, along with a model of the expected emission for a slice through a limb-brightened shell where the inner and outer radii listed in the figure give the best fit to the intensity of the edges of the nebula. Clearly it is plausible that additional emission fills its center — however, the kinematics of this nebula are unusual, as discussed below.

The outer limb-brightened edge of the equatorial ring allows us to measure its geometric parameters accurately. The major axis of the ring is $11\farcs1\pm0\farcs1$, while the minor axis is $7\farcs1\pm0\farcs1$. This yields an inclination of i=50.°2±1° if the ring is circular. The polar axis (corresponding to the direction of the minor axis on the sky) lies at P.A.=32.°4±1°. The intrinsic physical dimensions of the ring depend on the distance, which turns out to be somewhat surprising as discussed in §3.1.2.

Faint but visible in Figure 2*a* are a set of outer rings, another few arcseconds to the northeast and southwest. These remind one of the fainter outer rings around SN1987A, although they do not have the same special magnificence, appearing very thin, like butter scraped over too much bread. They give the impression of limb-brightened edges of faint bipolar lobes above and below the equatorial plane defined by the brighter inclined ring. In fact, the image of SBW1 in Figure 2*a* resembles the SN1987A model image of Martin & Arnett (1995) more closely than SN1987A itself does. This might lead one to suspect that the true geometry of SBW1 is akin to that of the bipolar model of Martin & Arnett. An even more extended, and fainter third set of rings or polar lobes may be present as well — these are hard to see on the printed page because of the grayscale levels in Figure 2*a*, but their emission can be seen at $\pm9''$ from the star in the intensity tracing along the polar axis of the nebula in Figure 3*a*. Deeper images may help reveal these putative outer rings, although they are nearly as faint as the fluctuations in the background nebula.

High-resolution spectra of SBW1 in Figures 5 and 6 clearly show extended nebular Hα and [N II] emission lines. The detailed kinematic structure of the emission along the slit shown in Figure 6 is rather bizarre. The strongest emission at the position of the main ring is redshifted to the northeast, and blueshifted to the southwest. The faint emission that fills the ring's interior in images follows the same general trend, but the detailed kinematic structure shows a triangular shape above and below the star in Figure 6. The emission does not converge on the star at the central position, as would be expected for a Hubble flow (homologous expansion), but rather, meets the position of the star at ±12 km s^{-1}. We offer no obvious explanation for this strange kinematic structure, except that it is marginally consistent with the interior of the ring being filled with a steadily outflowing flared disk. The cause of the triangular kinematic shape may be geometric, such that the motion of material was initially ejected or subsequently diverted out of the equatorial plane to form a flaring ring. In that case, the centroid of this emission at ±12 km s^{-1} implies a radial expansion speed for the ring and disk of roughly 19±2 km s^{-1} when it is corrected for the inclination angle of 50.°2. This expansion speed is identical to the radial expansion speeds of the rings around the blue supergiants Sher 25 and HD168625.

3.1.2. The central star and its distance

Figure 8 shows the spectrum of the central star of SBW1, which exhibits a spectral type of B1.5 Iab. The luminosity class is not entirely clear, because higher dispersion (Fig. 5) shows that the Balmer absorption lines are partially filled-in with nebular emission. The extracted spectrum of the bright central star in Figure 5*c* shows some nebular emission rising above the continuum level in Hα and double-peaked in the [N II] λ6583 line, superposed on a smooth continuum spectrum with prominent broad Balmer absorption. Despite the nebular contamination, a spectral type of B1.5 Iab seems likely. The luminosity class has two important ramifications concerning implications for stellar evolution, as well as the distance to SBW1.

First, it means that the central star is a massive star with an initial mass of roughly 18–25 $M_{\odot}$, and the ring is therefore an example of a pre-supernova environment much like that around SN1987A. The spectral type of B1.5 Iab justifies a close comparison to both Sher 25 (B1.5 Ia; Moffat 1983) and the progenitor of SN1987A (B3 I; Walborn et al. 1989), as well as permitting a link to the B[e] supergiants because of the emission line spectrum (see §4.2).

Second, the high luminosity suggests a distance much larger than 2.3 kpc, meaning that it is seen through the Carina Nebula and is projected within its boundaries only by chance, as if it wants to be found there. The absolute visual magnitude of a B1.5 Iab supergiant should be about −7.0 (Crowther et al. 2006), and the observed visual magnitude is roughly m_V=12.7 (Table 1). If SBW1 were located at 2.3 kpc in the Carina Nebula, the required total line-of-sight extinction would be very large at $A_V \simeq$7.9 magnitudes. Such high extinction is plausible, at least in principle, since SBW1 is seen along the same sight-line as dense molecular gas and dust associated with the Carina Nebula (Zhang et al. 2001; Grabelsky et al. 1988; Smith et al. 2000). However, the 2MASS colors (J=10.55, H=10.18, and K=9.95) suggest that the visual extinction is more like 3-5 magnitudes, depending on the extinction law. This implies that the star appears faint for its luminosity class because it is actually at a much farther distance.

In fact, the observed radial velocity of SBW1 also implies a much larger kinematic distance that places it in the far Carina arm. The systemic velocity in Figure 6 is redshifted from the centroid of nebular emission in Carina by roughly +30 km s^{-1}. The heliocentric radial velocity of η Carinae and the Carina Nebula is –8.1 km s^{-1} (Smith 2004), but that of SBW1 is +22±4 km s^{-1}, or an LSR velocity of roughly 10±4 km s^{-1}. The Carina Nebula is seen near the tangent of the Sagittarius-Carina spiral arm (e.g., Bok 1959), and a positive radial velocity at its position places SBW1 outside the solar circle on the far side of the Milky Way. The corresponding distance at a longitude of l=287° for a flat rotation curve is ∼7 kpc.[5]

This larger distance joins SBW1 to a string of other famous hot supergiants with circumstellar nebulae in the far Carina arm, seen on either side of the Carina Nebula, such as Sher 25 in NGC3603, AG Carinae, Hen 3-519, and HR Carinae. The massive cluster Westerlund 1 is also thought to be at a similar distance in this part of the Galactic plane. SBW1 is less conspicuous than these stars and its ring has not been discovered until now because of its much higher extinction column along its line of sight through dust and gas in the Carina Nebula, or perhaps, simply because it is overshadowed by other spectacular objects in the brighter inner parts of the nebula. At 7 kpc, the required extinction for its apparent magnitude is roughly 5

[5]But we may yet be deceived. There is some hint in our [O III] images and long slit spectra that the ring may be seen in silhouette against the background nebular emission. If true, this would mean that SBW1 must be located within the Carina Nebula after all and that its radial velocity is anomalous, unless there is another H II region projected behind Carina. Higher signal to noise data of the same type or possibly UV spectroscopy of absorption line profiles to the star may resolve this ambiguity. If SBW1 is far beyond Carina, the far (receding) side of the H II region should be seen in absorption. Thus, there are still questions that need answering.

magnitudes. This is in much better agreement with the extinction implied by near-IR photometry as noted above. Also, the larger distance of 7 kpc means that the ring's radius is about 0.19 pc — almost identical to the rings around SN1987A and Sher 25. With a radial expansion speed of 19 km s^{-1}, its dynamical age is $\sim 10^4$ yr. This age, too, is comparable to the rings around SN1987A and Sher 25.

Its high luminosity and circumstellar ring make SBW1 an object of considerable interest, and its similarity to the equatorial ring around SN1987A hints at some things which have not yet come to pass. The central star deserves further observations and analysis, such as monitoring for photometric and spectroscopic variability (i.e. is it an eclipsing or spectroscopic binary?), as well as detailed atmospheric spectral analysis to accurately determine its physical parameters. This is important if SBW1 is a potential supernova progenitor.

3.1.3. Size, mass, and chemical abundances

Table 2 lists line intensities for SBW1, corrected for a reddening value of $E(B-V)$=1 that would correspond to our estimate of $A_V \simeq 5$, adopting the value of R=4.8 that is appropriate for extinction in the direction of Carina (e.g., Smith 2002). From the red [S II] $\lambda\lambda$6717,6731 doublet, we measure an electron density of n_e=513 cm^{-3}, and from the ratio [N II] λ6548+λ6583/λ5755 we find an upper limit to the electron temperature of T_e <12,350 K. In the extracted EMMI spectrum of the nebula (Fig. 5*b*) we measure a [N II] λ6583/Hα intensity ratio of 0.483, which is within a few percent of the value we measure from RC Spec data. This would yield a N^+/H^+ abundance of $>1.6\times10^{-5}$ for an upper limit of T_e <12,350 K, or $N^+/H^+ \simeq 2.7\times10^{-5}$ for a more likely temperature of T_e=10,000 K. This is still *lower* than the solar abundance level; the nitrogen abundance would be roughly solar if the electron temperature were as low as 7,000 K (note, however, that this is only the abundance of N^+). The electron temperature would need to be roughly 5000 K or less, or there would need to be a large neutral N fraction compared to hydrogen in order for this ratio to suggest a considerable N overabundance in the ring. Therefore, our data are consistent with no significant N enrichment in the ring of SBW1. This lack of distinct nitrogen enrichment implies that SBW1 *has not yet passed through a red supergiant phase*, much like its twin Sher 25 (Smartt et al. 2002). Thus, in both these cases the equatorial rings must have been ejected when the stars were blue supergiants. This has important implications for the rings around SN1987A (Smith 2007; Smith & Townsend 2007).

If the ring is fully ionized, we can estimate its mass from the electron density and its apparent geometry in images. If we approximate the geometry of the ring as a torus, then at a distance of 7 kpc, the ring's radius is $R \simeq 0.19$ pc or 5.9×10^{17} cm, and the radius of its cross-sectional area is $r \simeq 5.3\times10^{16}$ cm ($\sim 0\farcs5$). Then assuming pure H gas, the ring's mass would be

$$M \simeq 2\pi^2 r^2 R\, m_H\, n_e\,. \tag{1}$$

With n_e=513 cm^{-3} (Table 2), we find M$\approx$0.014 $M_\odot$. This is probably a lower limit to the total mass, however, because we have neglected any neutral fraction or dense clumps, and we have ignored the mass of the disk interior to the ring, which may be comparable to the ring itself. This mass is comparable to the range of masses inferred for the few hundred AU disks around B[e] supergiants (Zickgraf et al. 1986). The largest mass known in a B[e] star disk is about 0.3 $M_\odot$ around R126 (Kastner et al. 2006). It is also comparable to the mass for the rings around RY Scuti (Smith et al. 2002b).

It would be interesting to measure the thermal-infrared flux from SBW1, in order to measure its dust

mass. Our long-slit spectra obtained with RC Spec hint that significant dust may be present in the nebula, since it is apparently seen in silhouette, blocking light from the background nebula in some emission lines (the low signal to noise and foreground emission preclude an accurate estimate of the dust mass, however).

3.2. Imaging and Spectroscopy of SBW2

The structure of SBW2 is far less orderly than SBW1. It is much fainter, more diffuse and ratty-looking, less symmetric, and it lacks a clear outer edge. The most unnatural and curious property, however, is that there is no obvious bright star near its center. There are three faint stars inside the ring (with $R \simeq$18.5, 20.5, and 20.7 mag), as well as a few extremely faint stars that are scarcely detected in our Magellan image with R of about 26 to 27. However, none of these stars is at the ring's center, and none stands out as an obvious candidate for a central star that may have ejected it. The sound crossing time of the ring is only a few tens of thousands of years. Any white dwarf at that young age should be several magnitudes brighter at visual wavelengths than these stars (e.g., Bergeron et al. 1995) if SBW2 is within the Carina Nebula at 2.3 kpc. Thus, the central star in SBW2 might avoid being seen if it were older, but to disappear entirely, that is a rare gift. Is the central object completely obscured by its own dust? Probably not, as we should see the outside of such an envelope ionized by whatever ionizes the rest of the ring. Perhaps the most likely – if unsatisfying – explanation is that a tight binary system was disrupted when one of the stars shed a large fraction of the system's mass. The origin of the ring and its invisible star system has since passed out of all knowledge, but proper motions of stars in the surrounding field may be quite illuminating.

The purpose of the intensity tracing in Figure 3*b* is to illustrate that SBW2 is not a limb-brightened spheroidal shell, but an actual flattened ring with a cleared interior. The intensity tracing through the minor axis of the nebula shows that the brightness in the middle of the ring drops to roughly zero. On the other hand, the dotted line in Figure 3*b* shows a model of the brightness distribution we would expect for a limb-brightened shell with a thickness corresponding to the apparent ring thickness in images. It is clear that the central region of the nebula would be more filled-in if it were a limb-brightened shell, unless the ring were much thinner than observed. Thus, the morphology of SBW2 is that of a flattened equatorial ring with a hollow center, titled at an inclination angle of about 52°. The average radius of the ring is $19\farcs8$, or 0.22 pc if it is in the Carina Nebula at 2.3 kpc. This makes its average radius only 10% larger than the equatorial ring around SN1987A (the inner and outer radii of SBW2 are roughly 0.16 and 0.25 pc, respectively).

Another unusual or unexpected property of SBW2 is that the brightest parts of the ring are not at the southeast and northwest tangent points along the major axis, as would be expected from limb-brightening in an optically-thin ring like SBW1. In fact, the brightness distribution is the opposite — the brightest parts of SBW2 are the near and far sides along the *minor* axis. This points to a high degree of azimuthal asymmetry in the system, perhaps implying that an eccentric binary system played a role in shaping the ejecta.

Although SBW2 is projected within the boundaries of the star-forming Carina Nebula, it is unlikely that this is a normal pre-main-sequence circumstellar envelope. In our experience, no pre-MS stars or protostars are surrounded by circumstellar disks that look anything like SBW2. They either have a bright central star with a bipolar reflection nebula or jets, or if the central star is obscured, it is because it is seen behind a dark, edge-on obscuring lane like in HH30 (Burrows et al. 1996; Stapelfeldt et al. 1999), HK Tau (Stapelfeldt et al. 1998), HV Tau C (Stapelfeldt et al. 2003), and several other reflection nebulae in Taurus and Orion (Padgett et al. 1999). This is clearly not the case here. In some situations like debris disks around Vega-like stars, images of the circumstellar disks may resemble SBW2, but they all have bright central stars that overwhelm

the nebula in optical images (e.g., Schneider et al. 1999; Fukagawa et al. 2004; Greaves et al. 1998).

This speculation is borne-out when we consider the spectrum of SBW2, and the chemical abundances it implies. The spectrum is shown in Figure 7*b*, with line intensities listed in Table 2. The strong [N II] lines relative to Hα immediately raise suspicion that the gas is nitrogen rich. (It also means that our Hα image in Figure 2*b* is actually a [N II] image.) With n_e of $\sim$280 cm^{-3} and an upper limit of T_e <14,900 K (Table 2), we find a lower limit of $n(N^+)/n(H^+)>1.35\times10^{-4}$, or about 1.5 times the solar abundance of N. For a more likely temperature of $T_e \lesssim$10,000 K, the nitrogen abundance would be $\gtrsim$4 times solar, and this is only for N^+. Thus, the gas in SBW2 is clearly nitrogen rich, and it is therefore the result of post–main-sequence mass loss, probably from an intermediate-mass progenitor star. Since the Carina Nebula H II region is only about 3 Myr old, this object must be an interloper, passing through the nebula instead of having been born there. The lack of any ionizing source within the ring argues strongly that it is within the Carina Nebula, and not just projected along the same sightline, like SBW1.

The emitting layer thickness of the ring seems to be roughly $l \simeq 2\times10^{17}$ cm (corresponding to a projected width of $\sim5''$; see Fig. 2*b*). With a density of n_e=280 cm^{-3} indicated by the [S II] lines (Table 2), it requires an incident flux of ionizing photons of $l\alpha_B n_e^2 > 10^{9.6}$ s^{-1} cm^{-2} in order to be fully ionized ($\alpha_B=2.6\times10^{-13}$ cm^3 s^{-1} is the case B recombination coefficient). At a projected radius of 70′ or $\sim$45 pc from the central ionizing clusters of the Carina Nebula, the ambient Lyman continuum flux near SBW2 would be roughly $Q_H/(4\pi d^2) \simeq 10^{9.6}$ s^{-1} cm^{-2} as well (Smith 2006). Thus, the star clusters of the Carina Nebula supply sufficient radiation to keep SBW2 fully ionized. This argues that SBW2 is, in fact, located within the Carina Nebula itself and not just projected along the same sightline by chance. If our assumption that SBW2 is fully ionized is incorrect, and that only its outer surface is ionized, then the required ionizing flux goes down. While the nebula is ionized, it lacks detectable [O III] emission in our images (not shown).

Assuming that SBW2 is fully ionized, we can provide a lower limit to its mass using the same technique as we did for SBW1. Using equation (1), but with $r=1.7\times10^{17}$ cm (4.″9) and $R=6.6\times10^{17}$ cm (0.22 pc) from Figure 2*b*, and n_e=280 cm^{-3} from Table 2, we find a total mass of $\sim$0.1 $M_\odot$ of ionized gas.

3.3. Imaging and Spectroscopy of SuWt2

This exotic ring nebula is shown in Figure 9*a*, which is an Hα+[N II] image obtained with the MOSAIC2 camera on the CTIO 4m telescope. This image shows considerably more detail than the discovery plates (Schuster & West 1976). From the image in Figure 9*a* we measure an inclination angle of 64°($\pm$2°), and from Figure 9*b* we find an average radius of 40.″5 or about 0.2 pc at a distance of 1 kpc, making it yet another ring with roughly the same radius as that of SN1987A's ring. As was the case for SBW2, an intensity tracing across SuWt2 (Figure 9*b*) shows that it is not a limb-brightened ellipsoidal shell, but instead is an actual flattended equatorial ring. A shell model would require substantially more flux in the center of the nebula than is seen in this image. Rather than being partially filled in, SuWt2 has faint excess flux *outside* the ring, suggesting that the ring may be the inner edge of a swept-up disk. The central star of SuWt2 has been found to be a 4.91-day eclipsing binary composed of 2 A-type stars of roughly 2.5 $M_\odot$ each (Bond 2000; Bond et al. 2002), where the inclination is in rough agreement with our estimate of the inclination of the ring nebula.

Figure 7c shows the red spectrum of the ring nebula, and Table 2 lists measured line intensities corrected for $E(B-V)$=0.25. We do not have a reliable estimate of $E(B-V)$ for SuWt2, but this reddening value is roughly what is needed to make the observed stellar colors consistent with an A-type photosphere. The strong nitrogen lines indicate that the Hα+[N II] image is dominated by [N II] λ6583 emission, and hint at an

enhanced N abundance. With $n_e \simeq 100$ cm^{-3} (the observed [S II] lines are close to the low density limit) and T_e=11,400 K from the [N II] line ratio, the observed [N II] λ6583/Hα ratio indicates $n(N^+)/n(H^+) \simeq 2.5 \times 10^{-4}$, or almost 3 times the solar abundance of N. Again, this is only for N^+, so the true N abundance could be higher. The presence of nitrogen-rich ejecta confirms that SuWt2 is a post–main-sequence object, and suggests that it had an intermediate-mass progenitor star. This is curious, given that the central star system of SuWt2 is observed to be an eclipsing binary of two A-type main-sequence stars.

Except for their central stars, SuWt2 and SBW2 are near twins. Again, we find that the ionization of this ring is rather suspicious. Ionized gas in the ring nebula requires a stronger flux of ionizing photons than can be supplied by two A-type stars. Bond et al. (2002) hypothesized that there may be a third star in the system — probably an unseen white dwarf — to account for the necessary UV flux. However, this white dwarf would need to be in a wide orbit, detached from the A+A eclipsing binary, and would therefore not be able to strongly affect the shape of the ring.

However, here we note a speculative alternative. Figure 9 also shows a bright star about 1′ east/northeast of SuWt2. This is the B2 star SAO 241302. It could supply the required ionizing photons if the two are at the same distance, following the same reasoning as above for SBW2 in Carina. This may seem at first to be rather fortuitous. However, we note that the Hα image of SuWt2's ring in Figure 9 shows an asymmetric brightness distribution. In particular, the ring is brighter on the east/northeast side — exactly on the side facing the bright B star. Thus, much like SBW2 in Carina and possibly also Sher 25, the nebula may be *externally illuminated* by a nearby hotter star. This possibility requires further investigation.

3.4. Imaging and Spectroscopy of WeBo1

This ring-shaped planetary nebula is located near the star forming region W4 in the Perseus arm of our Galaxy, about 5′ southwest of the X-ray binary LS I +61°303 (WeBo1 was discovered serendipitously while studying this source; Bond et al. 2003). It surrounds a Barium star and suspected white dwarf that may be the source of ionizing photons for the nebula. Bond et al. (2003) proposed that the equatorial ring was ejected during the tidally-locked AGB phase of the more massive star in the binary before it became a white dwarf, and that some of the AGB wind was accreted onto the companion star that is seen today as a rapidly-rotating Barium star. Thus, while the star shows no eclipses or orbital reflex motion that have been detected yet, the atmospheric chemical abundances give a strong indication that close binary evolution played a role in the axisymmetric mass loss.

3.4.1. New Results

Figure 10*a* shows an Hα image of the ring obtained with the ARC 3.5 meter reflector. The ring has a sharp inner edge with a radius of about 25″. As noted already by Bond et al. (2003), the lack of emission in the ring's interior means that it is a toroid and not a limb-brightened ellipsoidal shell. The major to minor axis ratio of 3.85 implies that the ring is close to edge-on with an axis of symmetry inclined by 75°±3° with respect to the line of sight. In contrast to the sharp inner boundary, the outer edge of the ring is diffuse, much like SBW2 and SuWt2.

The line intensities in Table 2 are measured from the spectra in Figures 10*b* and *c*. The higher resolution Keck spectrum was used for the relative intensities of [N II] λ6548 and λ6583 because they were better sepa-

rated from Hα than in the lower resolution DIS spectrum. The observed line intensities have been corrected for $E(B-V)$=0.57 (Bond et al. 2003). Table 2 also lists the electron density, electron temperature, and N^+/H abundance calculated from these ratios. The red [S II] lines are unusually weak in the spectrum, and unfortunately, the corresponding larger uncertainty in their intensities introduces a factor of $\sim$2 uncertainty in the electron density. The critical [N II] λ5755 line is also very weak, with a marginal 2σ detection that we regard as an upper limit. This indicates an upper limit to the electron temperature of $\lesssim 10^4$ K, which seems reasonable enough. From these values and the strength of [N II] λ6583, we find a $N^+/H^+ \gtrsim 10^{-4}$, indicating that the nebular gas is strongly enhanced in nitrogen, well above the solar value. This points toward an intermediate mass AGB progenitor star, just as in the case of SBW2 and SuWt2.

Interestingly, we see weak emission from He I λ5876 and [Ar III] λ7136 in the spectrum. These high ionization lines cannot be caused by radiation from the cool central star that dominates the visual spectrum, requiring either a hot white dwarf or an external source of ionization. We note that WeBo1 is found in the outskirts of the giant H II region W4, and is near the famous microquasar and radio emitting X-ray binary LS I +61°303. This proximity is intriguing, although the morphology in the [O III] image presented by Bond et al. (2003) seems to suggest a centrally-located ionizing source.

4. DISCUSSION

4.1. Comparison with Other Rings

SN1987A: Probably the most famous equatorial ring associated with post–main-sequence evolution is the remarkable equatorial ring around SN1987A. It was discovered shortly after being flash-ionized by the supernova, and eventually became the subject of intense study with *HST* (Crotts, Kunkel, & McCarthy 1989; Lundqvist & Fransson 1991; Jakobsen et al. 1991; Plait et al. 1995; Burrows et al. 1995; etc.). Now is a particularly interesting time for study of SN1987A, as the supernova blast wave is overtaking the circumstellar ring and causing a host of phenomena that are of great interest to shock evolution (Luo & McCray 1991; Chevalier & Dwarkadas 1995; Borkowski et al. 1997; Michael et al. 2000; Pun et al. 2002; Smith et al. 2005*b*). The appearance of a number of hotspots around the ring (Sonneborn et al. 1998; Michael et al. 2000; Pun et al. 2002; Sugerman et al. 2002) make it look like a pearl necklace. These spots show that while the ring appeared fairly smooth in images before it was struck by the shock, it had actually been shaped by Rayleigh-Taylor instabilities (Michael et al. 2000). The nebula around SN1987A is usually assumed to have been ejected during a previous red-supergiant phase and then swept-up by a blue supergiant wind. The ring itself is thought to be a swept-up thin disk that formed in the RSG wind as a consequence of close binary activity – possibly even a merger (Blondin & Lunqvist 1993; Martin & Arnett 1995; Morris & Podsiadlowski 2006; Collins et al. 1999). However, the larger outer rings that compose the triple-ring system around SN1987A still seem to defy explanation. Soker (2002) hypothesizes that these rings formed from precessing jets, while Morris & Podsiadlowski (2006) suggest that they are a natural consequence of a binary merger event. In any case, they are bona fide rings and not just limb-brightened edges of an hourglass (Burrows et al. 1995). Interestingly, our image of SBW1 in Carina looks more like one of these hourglass nebula simulations intended for SN1987A (see for example Fig. 5 in Martin & Arnett 1995).

Sher 25: The nebula around this B1.5 supergiant in NGC3603 (Sher 1965; Moffat 1983) is often held up as the Milky Way's "twin" of SN1987A's progenitor. Sher 25 has an equatorial ring that is reminiscent of the one around SN1987A (Brandner et al. 1997). However, Sher 25 is more luminous than Sk –69°202. With $\log(L/L_\odot)$=5.9 (Smartt et al. 2002), Sher 25 is probably too luminous to have gone through a red supergiant

phase. In fact, Smartt et al. find that the observed N/O abundance is incompatible with Sher 25 having been a RSG, and that the nebula was probably ejected as a blue supergiant. Furthermore, the spectrum of Sher 25 does not show the broad lines we would expect from an extremely rapid rotator that should be the product of a merger event (e.g., Morris & Podsiadlowski 2006). Thus, the similarity of its nebula to that around SN1987A may pose some difficulties for the RSG/merger scenario for the shaping of SN1987A's nebula. Our new discovery of SBW1 provides yet another twin of Sher 25 and SN1987A. SBW1 has the same radius as the rings around Sher 25 and SN1987A, and the central star is also a B1.5 supergiant (although it is less luminous than Sher 25, with a luminosity class of Iab instead of Ia). It also lacks the strong N-enrichment required for post-RSG evolution.

HD168625: The equatorial ring around this LBV candidate was discovered by Hutsemékers et al. (1994), and has been studied by several authors since then. In a recent study (Smith 2007) we discovered rings in a larger bipolar nebula seen in *Spitzer* images, making the nebula the nearest Galactic analog of the triple-ring system around SN1987A. The detection of an analog to SN1987A's nebula around an LBV is significant, because it provides a precedent that massive stars can eject rings+bipolar nebulae in LBV outbursts as blue supergiants rather than as RSGs. Elsewhere (Smith 2007) we have discussed this object in more detail, along with strong implications for the progenitor of SN1987A.

RY Sct: This is a massive 11-day eclipsing binary system in a state of overcontact (Milano et al. 1981), probably a WR+OB progenitor. Its unusual circumstellar nebula was first spatially resolved as a limb-brightened dust torus in the thermal-IR, where the compact torus had an apparent radius of only 1″ (Gehrz et al. 1995; 2001). The inner wall of this dust torus is ionized by the hot central stars, giving rise to strong radio continuum emission (Hjellming et al. 1973) and a peculiar, high-excitation emission-line spectrum (Merrill 1928; Smith et al. 2002b). The morphology of this ionized component of the nebula is remarkable — in high-resolution *HST* images it appears to be a pair of plane-parallel thin rings on either side of the equatorial plane (Smith et al. 1999). Proper motions indicate that the rings were ejected recently during an event sometime in the 19th century (Smith et al. 2001). The rings have radial expansion speeds of a little more than 40 km s^{-1} (Smith et al. 2002b). These ionized double-rings have half the radius of the larger dust torus, only 0.″5 or 900 AU at that distance. The inclination angle of the rings agrees to within a few degrees with the inclination angle of the orbit derived from the eclipsing light curve (Smith et al. 2002b; Milano et al. 1981), providing strong empirical evidence that the nebula and binary system share the same equatorial plane, and that close binary evolution plays an important role in shaping the nebula. RY Scuti is one of our best cases of a massive star caught in the act of shedding mass and angular momentum through its outer Lagrange point, probably an important step on its way toward becoming a colliding-wind WR+OB binary system. It argues strongly that equatorial rings can be the consequence of close binary evolution.

He 2-147: This equatorial ring nebula surrounds a binary system that is a symbiotic Mira. It was probably ejected in a symbiotic nova event about 300 yr ago, and currently shows a planetary nebula-like spectrum in the blue, and a cool supergiant spectrum in the red (Corradi et al. 1999, 2000). It is a close relative of bipolar symbiotic planetary nebulae like He 2-104.

Other clear examples of equatorial rings that are not as well studied as these are SuWt3, Abel 14, M1-41, Abel 47, and Lo 18 (see Schwarz et al. 1992). SuWt3 (Schuster & West 1976) is a remarkably clean, thin ring nebula that looks like a perfect ellipse, with $i \simeq 58°$ and R=28″. The distance to SuWt3 is not known, but R=0.14 pc × D_{kpc} makes it comparable to the other rings if the distance is around 1 kpc. Another intriguing object that deserves further study is the planetary nebula Abel 14 (Schwarz et al. 1992). It shows what seems to be a pair of plane-parallel rings above and below the equatorial plane, plus an outer torus component to the nebula (see Manchado et al. 1996). The appearance of the nebula is very similar to the

unusual double-ring nebula around RY Scuti (see above). Finally, there are still many more bipolar nebulae with less well-defined equatorial tori or rings at their waists, like η Car, He2-104, NGC 2346, NGC7027, MyCn18, and Abel 55.

4.2. Rings around B supergiants and a link to the B[e] supergiants

B[e] supergiants are luminous post-main-sequence stars that are characterized by IR excess emission from dust and prominent emission-line spectra, including the Balmer emission lines plus numerous lines of permitted and forbidden Fe^+ and other species (Zickgraf et al. 2003; Miroshnichenko et al. 2002). This emission is thought to arise in an outflowing circumstellar disk within a few hundred AU of the star (e.g., Zickgraf et al. 1986). Like the lower-luminosity Be stars, B[e] supergiants are thought to be rapid rotators.

B[e] supergiants have high luminosities, and occupy a similar area in the HR diagram as some of the less massive LBVs. However, unlike the LBVs, B[e] supergiants typically do not exhibit marked photometric or spectroscopic variability. Perhaps they are an earlier phase immediately before the LBVs, where the star still has sufficient mass to insulate it from the near-Eddington LBV instability. There are some deviations from this trend, however, hinting that B[e] supergiants and LBVs may be related after all: R4 in the SMC is a B[e] supergiant that exhibits variability characteristic of the LBVs (Zickgraf et al. 1996). Interestingly, R4 is very close to HD168625, SBW1, and the progenitor of SN1987A on the HR diagram, with a presumed initial mass of $\sim$20 $M_\odot$ (Zickgraf et al. 1996). These similarities taken together with the equatorial ring geometry suggest a plausible connection between B[e] stars and more extended rings. Also, R4 demonstrates that even relatively low-luminosity blue supergiants (low luminosity, at least, compared to extreme LBVs like η Car) can be susceptible to instabilities that cause sporadic outbursts. If a significant IR excess from dust were detected in SBW1, it would support this connection because the B[e] star disks also contain dust.

We therefore propose a direct link between B[e] supergiants and the class of massive, early B supergiants surrounded by spatially-resolved ring nebulae (including SN1987A, SBW1, Sher 25, and HD168625). Specifically, we suspect that the outflowing disks in B[e] stars that emit their IR excess and bright-line spectra will continue to expand, and after a few thousand years will form spatially resolvable equatorial rings at $\sim 10^4$ AU from the stars. This would be analogous to the disk clearing that is thought to occur in lower luminosity Be stars (e.g., Meilland et al. 2006). This link, in turn, would suggest that in the massive ringed stars in our sample, rapid rotation rather than close binary evolution may shape their ejecta. Both Sher 25 and HD168625 have been studied, and no evidence for binarity has yet been reported, although renewed efforts would be of great interest. SBW1 should also be monitored to search for eclipses or radial velocity variations. Both Sher 25 and SBW1 are luminous hot supergiants that probably have *not* gone through a RSG phase, as noted earlier, while HD168625 is a luminous blue variable (LBV) candidate. Thus, the most plausible scenario for the formation of their rings is ejection by a rapidly-rotating star in an LBV eruption or some related episodic mass loss as blue supergiants (see Smith 2007; Smith & Townsend 2007). In this context, the fact that their nebulae are near twins of SN1987A is quite suggestive.

It is worth pointing out that the presence of descrete rings – as opposed to smooth thin disks – is evidence for recent temporal variability of the central star in each object, regardless of the specific interpretation for their formation. The presence of a ring requires either 1) a brief ejection episode as a blue supergiant, B[e] star, or LBV, where $\dot{M}$ increased drastically for a short time, or 2) the initial formation of a thin disk over a long timescale, which is then swept up into a ring following a sharp increase in the speed of the stellar wind. Both these mechanisms would require that the ejection of rings is a consequence of late stages of

stellar evolution, rather than normal main-sequence evolution.

In the context of linking spatially-resolved rings to B[e] supergiants, RY Scuti (Smith et al. 2002b) is perhaps one of the most interesting objects available for detailed study. It has a toroidal nebula, it shares many spectroscopic properties in common with the B[e] supergiants (Men'shchikov & Miroshnichenko 2005; Allen & Swings 1976; Smith et al. 1999), and it is an eclipsing binary in a state of overcontact that is known to be shedding mass and angular momentum. Its rings have a radius of 1000–2000 AU — in between the expected radii of emitting circumstellar material around B[e] stars (a few to several hundred AU) and most of the spatially-resolved rings discussed here at radii of a few $\times 10^4$ AU. The dust mass and IR excess of RY Scuti are similar to B[e] supergiants, although the grains are at a lower temperature around RY Scuti because they are farther from the star. The $\sim$40 km s^{-1} expansion speed of its rings (Smith et al. 2002) is typical of the narrow-line regions around B[e] stars (Zickgraf et al. 1986), but faster than the speeds of the more extended rings discussed in this paper, which have presumably decelerated. Thus, RY Scuti may represent a very short-lived "missing link" between the B[e] supergiants and the early B supergiants surrounded by rings.

4.3. The Role of Binarity

The sample of objects in Table 3 may yield interesting clues to the role of close binary interactions in the formation mechanism of circumstellar rings. Six of the nine objects are known to be or suspected to be close interacting binaries. RY Scuti, SuWt2, and He2-147 are definite eclipsing binaries, while the central star of WeBo1 is a Barium star that probably resulted from mass transfer in a Roche lobe overflow (RLOF) phase (Bond et al. 2003). The remaining two suspected binaries are somewhat unusual cases: SN1987A is thought to have undergone a binary merger event when the ring was ejected, as noted in §1 (although there may be problems with the merger interpretation; Smith 2007; Smith & Townsend 2007). The invisible central star in the SBW2 ring probably requires that a central binary system was disrupted and that the stars were ejected from the system, as discussed earlier in §3.2. Taken together, this collection of objects strongly suggests that mass loss through the outer Lagrangian point in a common-envelope/RLOF phase of close binary evolution is a preferred avenue for the forging of rings, at least for intermediate-mass systems. There are good reasons why more luminous massive stars can produce rings without close binary influence (Smith & Townsend 2007). RY Scuti is a key object in this regard, as it is currently caught in this brief but important RLOF phase and it is the only confirmed binary among the supergiants with rings. In a scenario where a massive star has a companion close enough and massive enough to shape its ejecta, it would be difficult for that companion to escape detection.

Forging of such rings through close binary interaction may be relevant for the formation of bipolar planetary nebulae if a fast wind expands into such an environment with a strong equatorial density enhancement. Some of the most tightly-pinched waists among bipolar planetary nebulae are seen in so-called symbiotic PNe, and several of these are strongly suspected to be binaries (e.g., M 2-9 [Doyle et al. 2000]; Mz 3 [Smith 2003]; Hb12 [Hsia et al. 2006]). However, several of the objects we discuss here are equatorial rings that are suspected to be present *before* the planetary nebula phase, and are only seen in rare circumstances as discussed next.

4.4. A Secret That Only Fire Can Tell: Are Equatorial Rings Commonplace?

Two-thirds of the objects in Table 3 (the two new objects discovered here, plus SN1987A, Sher 25, HD168625, and WeBo1) are seen projected in or near giant H II regions — environments that may provide a copious external source of UV photons (admittedly, the nebula of SN1987A was flash ionized by the supernova event itself). RY Scuti has a sufficiently hot and luminous star to provide its own UV illumination. SBW2 in Carina has no bright central star, but we have shown earlier that the hot stars that power the Carina Nebula can supply sufficient ionizing photons. SuWt2, with two A-type stars, may have a similar problem, with a nearby early B star providing a similar solution. WeBo1 is near W4 and the X-ray binary LS I +61°303. This raises the question of whether such rings around post-MS stars might be fairly common, but go unseen where there is a lack of favorable external illumination. Such precious rings may be the long sought-after doughnuts (e.g., Frank et al. 1998) needed for the interacting winds scenario of bipolar planetary nebula formation. Even if external ionization is not critical in making these rings visible, the fact that most of them are seen in close proximity to H II regions certainly increases their chances for serendipitous discovery.

This suggests that there may be many more rings of similar size and morphology surrounding post-MS intermediate-mass stars throughout the Galaxy, but they go undetected either because they are not illuminated or because most of the Galactic plane has not been surveyed with deep narrowband imaging as intensively as star-forming regions have been. Excluding the more massive stars in our sample, which may supply their own ionization and are probably found preferentially near H II regions anyway, we can make an order of magnitude extrapolation. H II regions occupy only 0.1–1% of the volume of the galactic disk, so there may be several hundred to a few thousand more dark rings in the Galaxy, comparable to the known number of planetary nebulae. This estimate is probably conservative, since not all galactic H II regions have been surveyed in detail. Thus, it is at least plausible that such a population of undetected rings could exist, and that these could play a role in binding the waists of bipolar planetary nebulae. Thus, such rings may partly answer the question "where's the doughnut" posed by Frank et al. (1998).

5. SUMMARY

5.1. SBW1 in Context

The discovery of the ring in SBW1 is the most interesting result of this study, because it adds to the small number of such rings known around blue supergiants that are likely supernova progenitors. In particular, the radius and morphology of the ring in SBW1 make it nearly identical to the equatorial ring around SN1987A, and the luminosity and spectral type of the central star are almost identical to Sk−69°202. The other two B supergiants with similar ring nebulae, Sher 25 and HD 168625, are both significantly more luminous than Sk−69°202. The low N abundance in SBW1, however, is surprising because it means that the star has not yet been a RSG, and so hot supergiants must be able to eject rings like this without a slow/fast interacting wind scenario. One intriguing possibility is that these rings correspond to older phases of ejected material that would have initially been seen closer to the star as a B[e] supergiant. If IR excess emission were detected in SBW1, it would add weight to this idea since B[e] supergiants have dusty disks or tori. The same may be true for Sher 25, HD168625, and the progenitor of SN1987A, while the much smaller radius rings around RY Scuti may suggest that it is in an intermediate phase. SBW1 should be monitored photometrically and spectroscopically to determine if it is a close binary system.

5.2. SBW2 in Context

In all respects, except for the troublesome fact that its central star is missing, SBW2 is a carbon copy of SuWt2 and WeBo1. These rings are associated with intermediate-mass (2-8 $M_{\odot}$) close binary stars. Their rings appear thicker and more diffuse, with inner edges that are sharper than their outer limits, as compared to the more elegant equatorial rings around the blue supergiant stars. Their radii around 0.2 pc are oddly similar to those surrounding the more massive stars. They all seem to be nitrogen rich, with [N II] λ6583 much brighter than Hα. All seem to lack a suitable source of ionizing photons, unless a hot white dwarf has gone undetected in each system. We have suggested that the lack of any bright central star in SBW2 may indicate that a binary system has been distrupted, which would be quite extraordinary, while the remaining rings in the intermediate-mass class all seem to be close binaries. Thus, in contrast to the massive stars with rings, at low/intermediate mass it seems more likely that close binary evolution rather than rapid rotation of single stars governs the forging of these rings. If they are detected only in these few cases because of selection effects or favorable ionization, such rings may be numerous in the Galaxy. As such, they could provide the pre-existing equatorial density enhancements needed to form bipolar nebulae through the interacting winds scenario.

We thank Steve Lawrence for kindly obtaining the blue spectrum of SBW1 for us, and Nolan Walborn for advice on its spectral type. We also thank Jon Morse for assistance on the Magellan observing run and Bo Reipurth for assistance with the Keck run. Partial support for N.S. was provided by NASA through grant HF-01166.01A from the Space Telescope Science Institute, which is operated by the Association of Universities for Research in Astronomy, Inc., under NASA contract NAS 5-26555. Additional support was provided by NSF grant AST 98-19820 and NASA grants NCC2-1052 and NAG-12279 to the University of Colorado.

REFERENCES

Allen, D.A., & Swings, J.P. 1976, A&A, 47, 293

Balick, B., & Frank, A. 2002, ARAA, 40, 439

Bergeron, P., Wesemael, F., & Beauchamp, A. 1995, PASP, 107, 1047

Bjorkman, J.E., & Cassinelli, J.P. 1993, ApJ, 409, 429

Blondin, J.M., & Lundqvist, P. 1993, ApJ, 405, 337

Bok, B.J. 1959, Observatory, 79, 58

Bond, H.E. 2000, in ASP Conf. Ser. 199, 115

Bond, H.E., O'Brien, S., Sion, E.M., Mullan, D.J., Exter, K., Pollacco, D.L., & Webbink, R.F. 2002, in ASP Conf. Ser. 279, 239

Bond, H.E., Pollacco, D.L., & Webbink, R.F. 2003, AJ, 125, 260

Borkowski, K., Blondin, J., & McCray, R. 1997, ApJ, 476, L31

Brandner, W., Grebel, E.K., Chu, Y.H., & Weis, K. 1997, ApJ, 475, L45

Burrows, C.J., et al. 1995, ApJ, 452, 680

Burrows, C.J., et al. 1996, ApJ, 473, 437

Chevalier, R.A., & Dwarkadas, V.V. 1995, ApJ, 452, L45

Collins, T.J.B., Frank, A., Bjorkman, J.E., & Livio, M. 1999, ApJ, 512, 322

Corradi, R.M., Ferrer, O., Schwarz, H.E., Brandi, E., & Garcia, L. 1999, A&A, 348, 978

Corradi, R.M., Livio, M., Schwarz, H.E., & Munari, U. 2000, ASP Conf. Ser. 199, Asymmetrical Planetary Nebulae II, ed. J.H. Kastner, N. Soker, & S. Rappaport (San Francisco: ASP), 175

Cranmer, S.R., & Owocki, S.P. 1995, ApJ, 440, 308

Crotts, A.P.S., & Heathcote, S.R. 1991, Nature, 350, 683

Crotts, A.P.S., & Heathcote, S.R. 2000, ApJ, 528, 426

Crotts, A.P.S., Kunkel, W.E., & McCarthy, P.J. 1989, ApJ, 347, L61

Crowther, P.A., Lennon, D.S., & Walborn, N.R. 2006, A&A, 446, 279

Cure, M., Rial, D.F., & Cidale, L. 2005, A&A, 437, 929

Doyle, S., Balick, B., Corradi, R.L.M., & Schwarz, H.E. 2000, AJ, 119, 1339

Frank, A. 1999, New AStron. Rev., 43, 31

Frank, A., & Mellema, G. 1994, ApJ, 430, 800

Frank, A., Ryu, D., & Davidson, K. 1998, ApJ, 500, 291

Fukagawa, M., et al. 2004, ApJ, 605, L53

Gehrz, R.D., et al. 1995, ApJ, 439, 417

Gehrz, R.D., Smith, N., Jones, B., Puetter, R., & Yahil, A. 2001, ApJ, 559, 395

Grabelsky, D.A., Cohen, R.S., Bronfman, L., & Thaddeus, P. 1988, ApJ, 331, 181

Greaves, J.S., Holland, W.S., Moriarty-Schieven, G., Jenness, T., Dent, W.R.F., Zuckerman, B., McCarthy, C., Webb, R.A., Butner, H.M., Gear, W.K., & Walker, H.J. 1998, ApJ, 506, L133

Hjellming, R.M., Blankenship, L.C., & Balick, B. 1973, Nature Phys. Sci., 242, 84

Hsia, C.H., Ip, W.H., & Li, J.Z. 2006, AJ, 131, 3040

Hutsemékers, D., Van Drom, E., Gosset, E., & Melnick, J. 1994, A&A, 290, 906

Ignace, R., Cassinelli, J.P., & Bjorkman, J.E. 1996, ApJ, 459, 671

Jakobsen, P., et al. 1991, ApJ, 369, L63

Kastner, J.H., Buchanan, C.L., Sargent, B., & Forrest, W.J. 2006, ApJ, 638, L29

Lamers, H.J.G.L.M., & Pauldrach, A.W.A. 1991, A&A, 244, L5

Latter, W.B., Dayal, A., Bieging, J.H., Meakin, C., Hora, J.L., Kelly, D.M., & Tielens, A.G.G.M. 2000, ApJ, 539, 783

Lunqvist, P., & Fransson, C. 1991, ApJ, 380, 575

Luo, D., & McCray, R. 1991, ApJ, 379, 659

Manchado, A., Guerrero, M.A., Stanghellini, L., & Serra-Richart, M. 1996, "The IAC morphological catalog of northern galactic planetary nebulae"

Martin, C.L., & Arnett, D. 1995, ApJ, 447, 378

Matt, S., & Balick, B. 2004, ApJ, 615, 921

Men'shchikov, A.B., & Miroshnichenko, A.S. 2005, A&A, 443, 211

Meilland, A., Stee, P., Zorec, J., & Kanaan, S. 2006, A&A, 455, 953

Merrill, P.W. 1928, ApJ, 67, 179

Michael, E., et al. 2000, ApJ, 542, L53

Milano, L., Vittone, A., Ciatti, F., Mammano, A., Margoni, R., & Strazzulla, G. 1981, A&A, 100, 59

Miroshnichenko, A.S., et al. 2002, A&A, 390, 627

Moffat, A.F.J. 1983, A&A, 124, 273

Morris, T., & Podsiadlowski, P. 2006, MNRAS, 365, 2

Owocki, S.P., Cranmer, S.R., & Gayley, K.G. 1996, ApJ, 472, L115

Padgett, D.L., Brandner, W., Stapelfeldt, K.R., Strom, S.E., Tereby, S., & Koerner, D. 1999, AJ, 117, 1490

Plait, P.C., Lundqvist, P., Chevalier, R.A., & Kirshner, R.P. 1995, ApJ, 439, 730

Pun, C.S.J., et al. 2002, ApJ, 572, 906

Sahai, R., et al. 1999, AJ, 118, 468

Schneider, G., et al. 1999, ApJ, 513, L127

Schuster, H.E., & West, R.M. 1976, A&A, 46, 139

Schwarz, H.E., Corradi, R.L.M., & Melnick, J. 1992, A&AS, 96, 23

Sher, D. 1965, MNRAS, 129, 237

Smartt, S.J., Lennon, D.J., Kudritzki, R.P., Rosales, F., Ryans, R.S.I., & Wright, N. 2002, A&A, 391, 979

Smith, N. 2003, MNRAS, 342, 383

Smith, N. 2004, MNRAS, 351, L51

Smith, N. 2006, MNRAS, 367, 763

Smith, N. 2007, AJ, 133, 1034

Smith, N., & Townsend, R.H.D. 2007, ApJ, in press

Smith, N., Egan, M.P., Carey, S., Price, S.D., Morse, J.A., & Price, P.A. 2000, ApJ, 532, L145

Smith, N., Gehrz, R.D., Humphreys, R.M., Davidson, K., Jones, T.J., & Krautter, J. 1999, AJ, 118, 960

Smith, N., Gehrz, R.D., & Goss, W.M. 2001, AJ, 122, 2700

Smith, N., Gehrz, R.D., Hinz, P.M., Hoffmann, W.F., Mamajek, E.E., & Meyer, M.R., & Hora, J.L. 2002*a*, ApJ, 567, L77

Smith, N., Gehrz, R.D., Stahl, O., Balick, B., & Kaufer, A. 2002*b*, ApJ, 578, 464

Smith, N., Bally, J., & Brooks, K.J. 2004, AJ, 127, 2793

Smith, N., Stassun, K.G., & Bally, J. 2005*a*, AJ, 129, 888

Smith, N., Zhekov, S.A., Heng, K., McCray, R., Morse, J.A., & Gladders, M. 2005*b*, ApJ, 635, L41

Soker, N. 2002, ApJ, 577, 839

Sonneborn, G., et al. 1998, ApJ, 492, L139

Stapelfeldt, K.R., Krist, J.E., Menard, F., Bouvier, J., Padgett, D.L., & Burrows, C.J. 1998, ApJ, 502, L65

Stapelfeldt, K.R., Menard, F.,Watson, A.M., Krist, J.E., Dougados, C., Padgett, D.L., & Brandner, W. 2003, ApJ, 589, 410

Stapelfeldt, K.R., et al. 1999, ApJ, 516, L95

Sugerman, B.E.K., Lawrence, S.S., Crotts, A.P.S., Bouchet, P., & Heathcote, S.R. 2002, ApJ, 572, 209

Townsend, R.H.D., & Owocki, S.P. 2005, MNRAS, 357, 251

ud-Doula, A., & Owocki, S.P. 2002, ApJ, 576, 413

Walborn, N.R. 1995, RevMexAA Ser. Conf., 2, 51

Walborn, N.R., Prevot, M.L., Prevot, L., Wamsteker, W., Gonzalez, R., Gilmozzi, R., & Fitzpatrick, E.L. 1989, A&A, 219, 229

Washimi, H., Shibata, S., & Mori, M. 1996, PASJ, 48, 23

Zhang, X., Lee, Y., Bolatto, A., & Stark, A. 2001, ApJ, 553, 274

Zickgraf, F.J., Kovacs, J., Wolf, B., Stahl, O., Kaufer, A., & Appenzeller, I. 1996, A&A, 309, 505

Zickgraf, F.J., Wolf, B., Stahl, O., Leitherer, C., & Appenzeller, I. 1986, A&A, 163, 119

Zickgraf, F.J., et al. 2003, A&A, 408, 257

This preprint was prepared with the AAS LaTeX macros v5.2.

Table 1. Two New Ring Nebulae in Carina

Name	α(2000)	δ(2000)	Apparent Size	Comments
SBW1	$10^{\rm h}40^{\rm m}19\overset{\rm s}{.}4$	-59°49′09″.7	11″.1×7″.1	V=12.7, R=12.14
SBW2	$10^{\rm h}36^{\rm m}09\overset{\rm s}{.}2$	-59°09′19″.2	37″×23″	(R=18.5, 20.5, 20.7)

Note. — For SBW1 these coordinates correspond to the bright central star, while the position for SBW2 corresponds to the approximate center of the ring, since no obvious bright star can be associated with it. V and R magnitudes of the stars are from the GSC 2.2 catalog.

Table 2. Dereddened Line Intensities[a]

λ(Å)	I.D.	SBW1	SBW2	SuWt2	WeBo1
5755	[N II]	<0.99	<17.1	11.3	$\lesssim$2.4
5876	He I	···	···	...	5.7
6300	[O I]	···	30.4	20.7	14.6
6312	[S III]	···	···	10.5	...
6364	[O I]	···	···	···	11.9
6548	[N II]	14.1	174	201	62.2
6563	Hα	100	100	100	100
6583	[N II]	46.2	568	620	201
6717	[S II]	6.82	31.1	46.3	4.7
6731	[S II]	6.56	26.9	34.8	4.1
		Derived (assumed) properties			
E(B-V)	···	(1.0)	(0.5)	(0.25)	(0.57)
n_e	[S II]	513 cm^{-3}	280 cm^{-3}	90 cm^{-3}	312 cm^{-3}
T_e	[N II]	<12,350 K	<14,900 K	11,400 K	$\lesssim$9,600 K
$n(N^+)/n(H^+)$	···	$>1.6\times10^{-5}$	$>1.35\times10^{-4}$	2.5×10^{-4}	$\gtrsim1.3\times10^{-4}$

[a]Intensities are given relative to Hα=100, and have been dereddened using R=3.1 and the listed $E(B-V)$ values. Uncertainties in fainter lines are typically 10%, but more for the faint lines in WeBo1. Upper limits are given for [N II] λ5755 in SBW1 and SBW2, while the value for WeBo1 is a marginal ($\sim2\sigma$ detection), which we regard as an approximate upper limit.

Table 3. Properties of Well-Defined Equatorial Ring Nebulae

Name	Radius	Inclination	V_{exp}[a]	Age (yr)	HII region	N rich?	Binary?	Comments
SBW1	0.19 pc	50.°2	19	9600	Carina	N	?	B1.5 Iab
SBW2	0.22 pc	52°	<8	>2.6(4)	Carina	Y	disrupted?	no star
SN1987A	0.21 pc	44°	10	2(4)	30 Dor	Y	merged?	B3 I; triple rings
Sher 25	0.20 pc	64°	20	9600	N3603	Y	...	B1.5 Ia
HD168625	0.09 pc	61°	19	4500	M17	Y	...	LBV; triple rings
WeBo1	0.24 pc	69°	?	...	W4	Y	mass transfer	Barium star
SuWt2	0.2 pc (D_{kpc})	64°	?	...	...	Y	eclipsing	A+A binary
He2-147	0.025 pc	55°	50	480	...	Y	eclipsing	symbiotic mira
RY Sct	0.005 pc	75°	43	110	...	Y	eclipsing	WR+OB; double rings

[a]This is the *radial* expansion velocity in km s^{-1} corrected for the inclination of the system.

References. — SN1987A: Plait et al. (1995); Crotts & Heathcote (2000) — Sher 25: Brandner et al. (1997) — HD168625: see Smith (2007) and references therein — WeBo1: Bond et al. (2003) — SuWt2: Schuster & West (1976) and this work — He 2-147: Corradi et al. (1999, 2000) — RY Sct: Smith et al. (1999, 2001, 2002*b*).

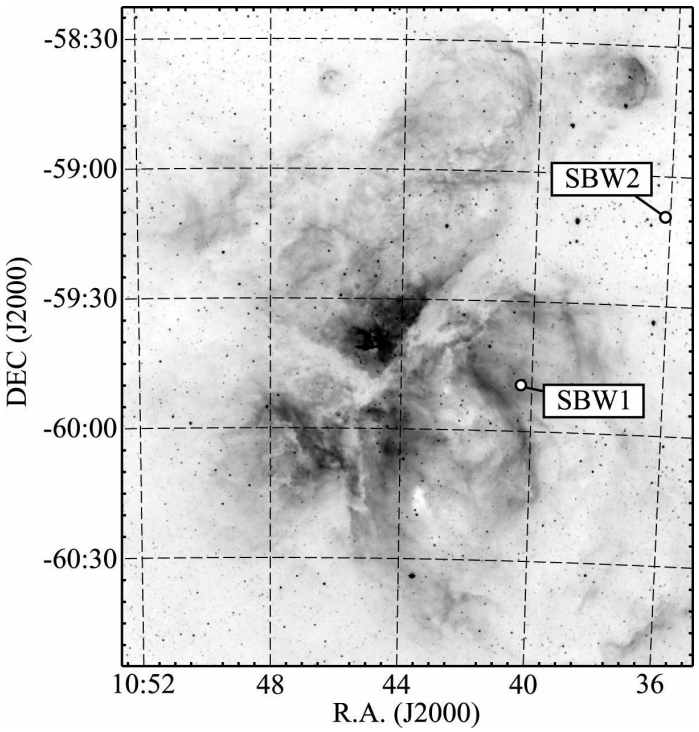

Fig. 1.— Large-scale Hα image of the Carina Nebula (from Smith et al. 2000) showing the locations of SBW1 and SBW2 relative to the rest of the giant H II region.

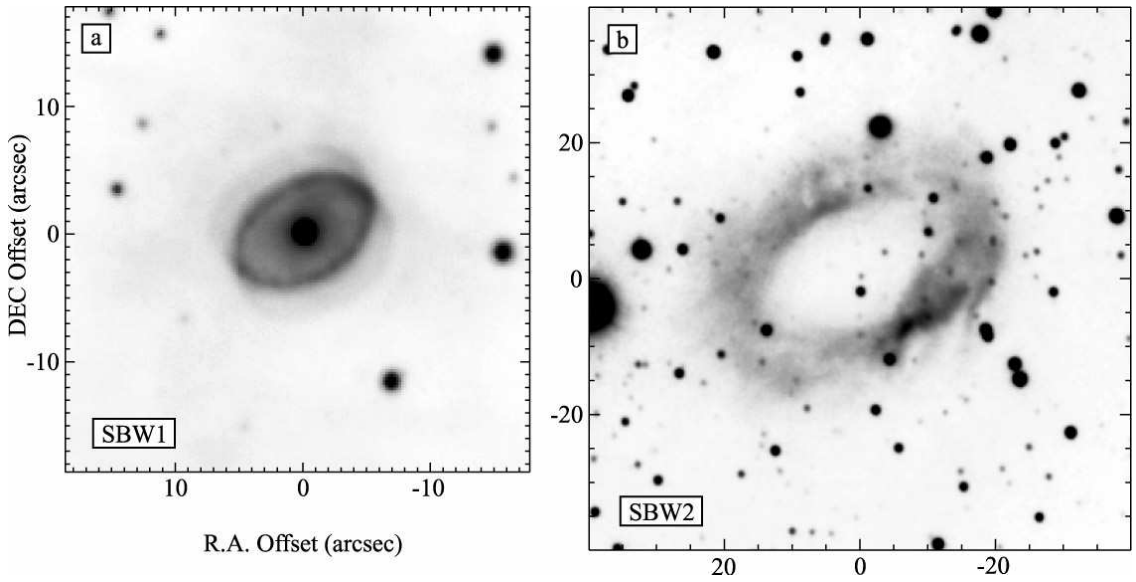

Fig. 2.— Magellan/MagIC Hα+[N II] images of SBW1 (a) and SBW2 (b). Note that the two images are not reproduced here at exactly the same size scale.

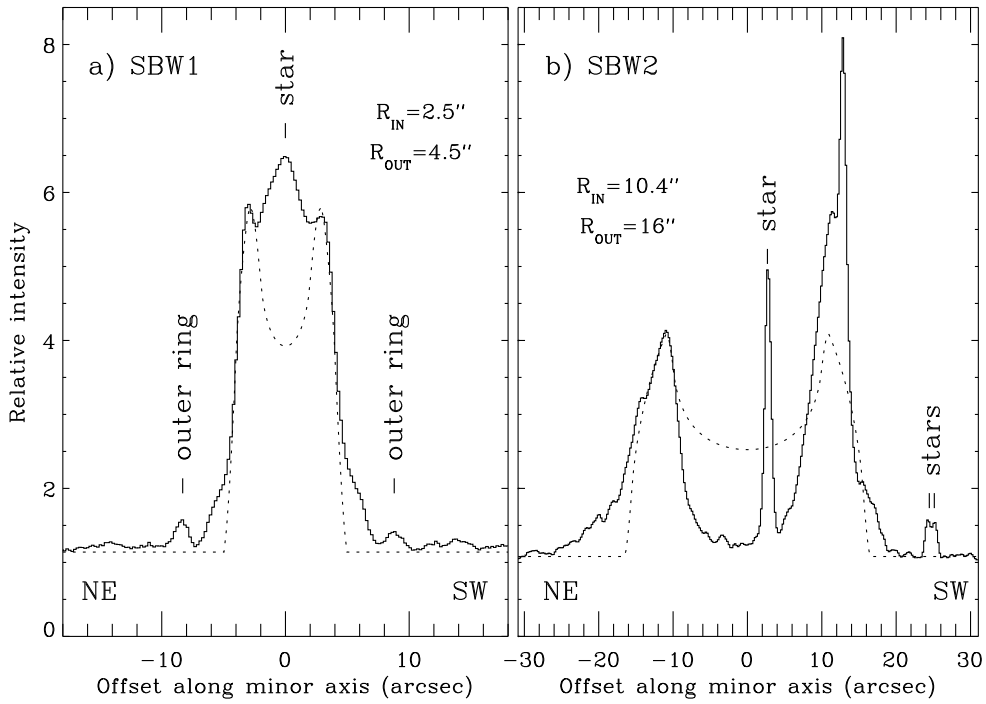

Fig. 3.— Intensity tracings across the images in Figure 2. (a) Tracing along the minor axis of SBW1, taken from two 0.″5-wide segments on either side of the EMMI slit aperture shown in Figure 4*a*, in order to avoid bright light from the star. (b) Tracing through the middle of SBW2, immediately to the northwest of the EMMI slit shown in Figure 4*b*. In each panel, the dashed line is a model for the expected emission from a cross section through a limb-brightened thin shell with the inner and outer radii listed in each panel. In Panel B, especially, it is clear that the observed emission is not consistent with the limb-brightened shell.

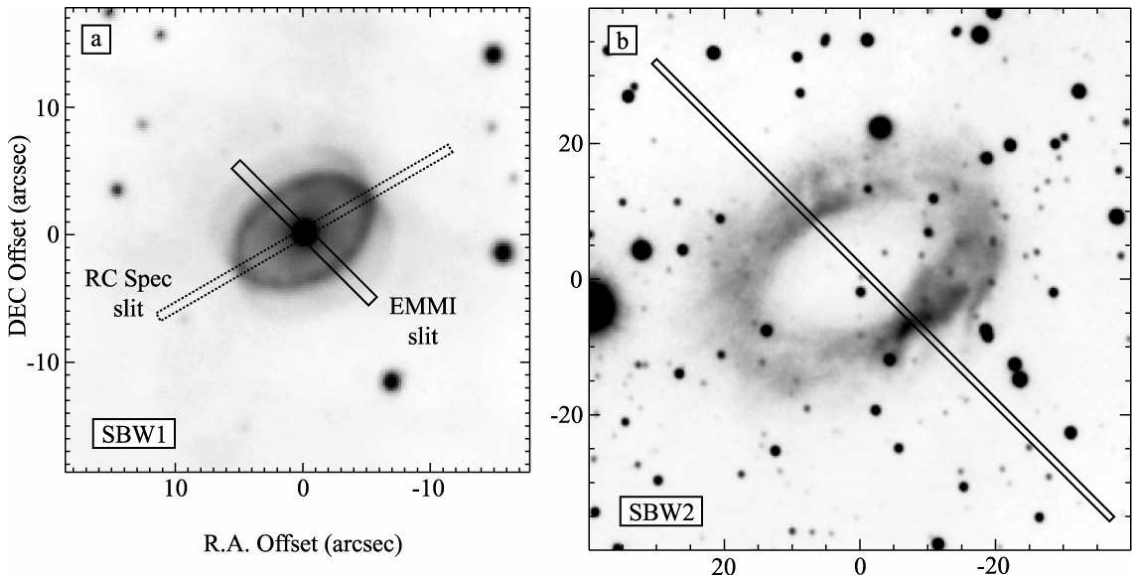

Fig. 4.— Same as Figure 2, but showing the EMMI and RC Spec slit positions.

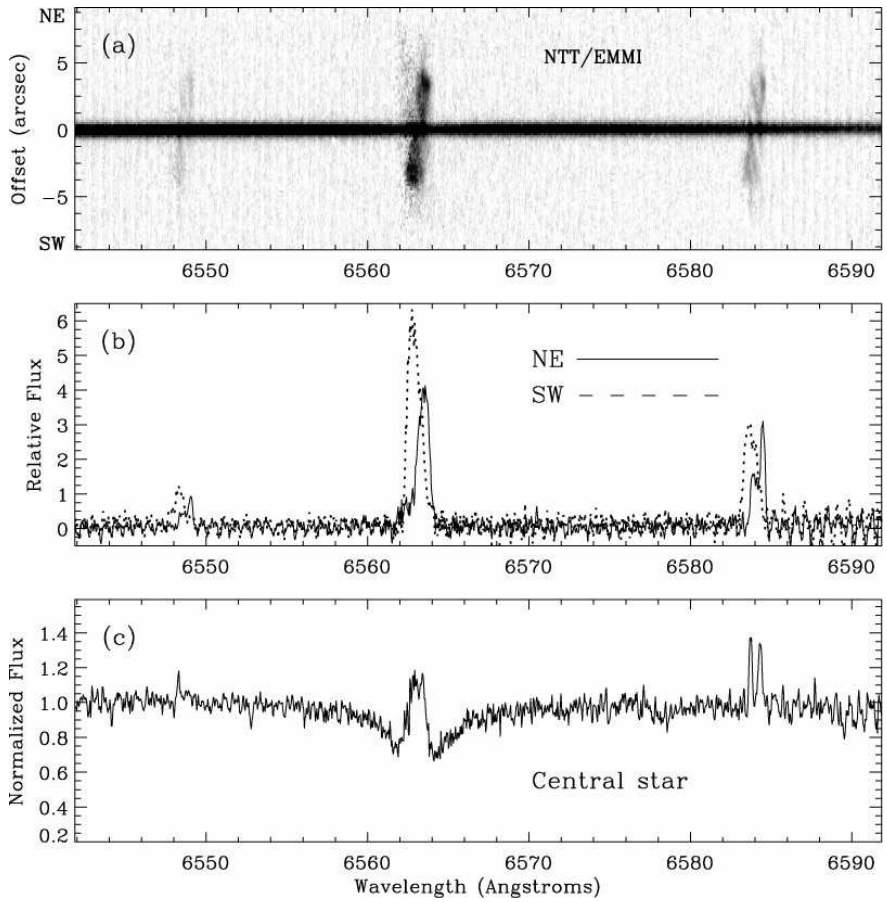

Fig. 5.— (a) Background-subtracted long-slit spectrum of SBW1 in the region near Hα, with the 15″ slit aperture of EMMI passing through the central star, oriented at P.A.=45° (NE is up and SW is down). (b) Intensity tracings of the nebular emission in Panel A, offset to the NE (solid) and SW (dashed). (c) Extracted spectrum of the central star in the same wavelength range; background H II region emission has been subtracted, but circumstellar nebular emission has not.

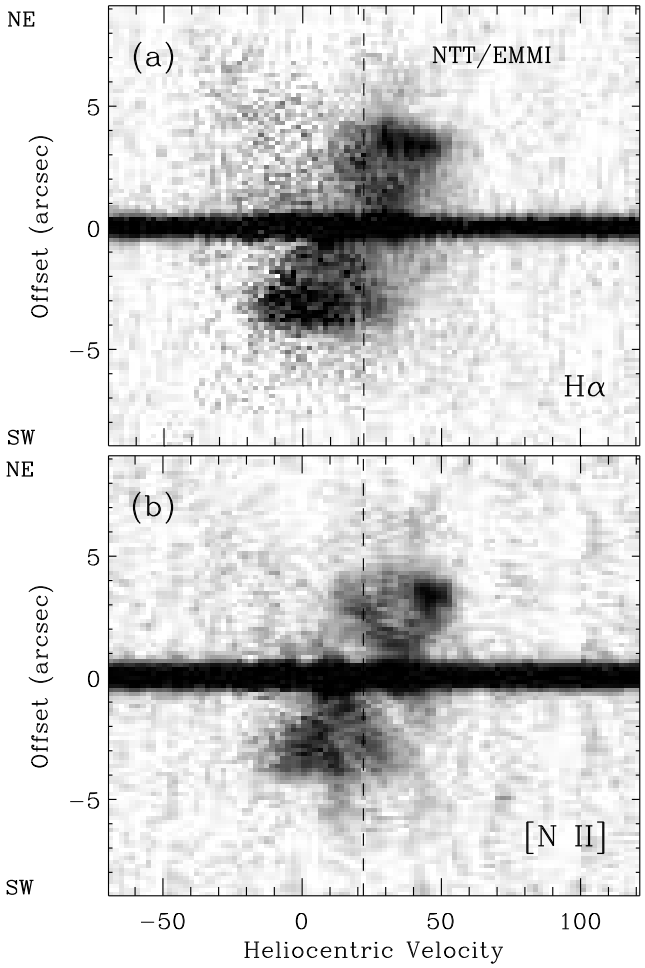

Fig. 6.— Long-slit nebular kinematics of SBW1 in (a) Hα and (b) [N II] λ6583. The velocity scale is heliocentric, and the dashed line marks the presumed systemic velocity at +22 km s^{-1}, which is offset by +30 km s^{-1} from the average emission velocity of gas in the Carina Nebula at −8.1 km s^{-1} (Smith 2004). These two panels are sections of the data in Figure 5*a*.

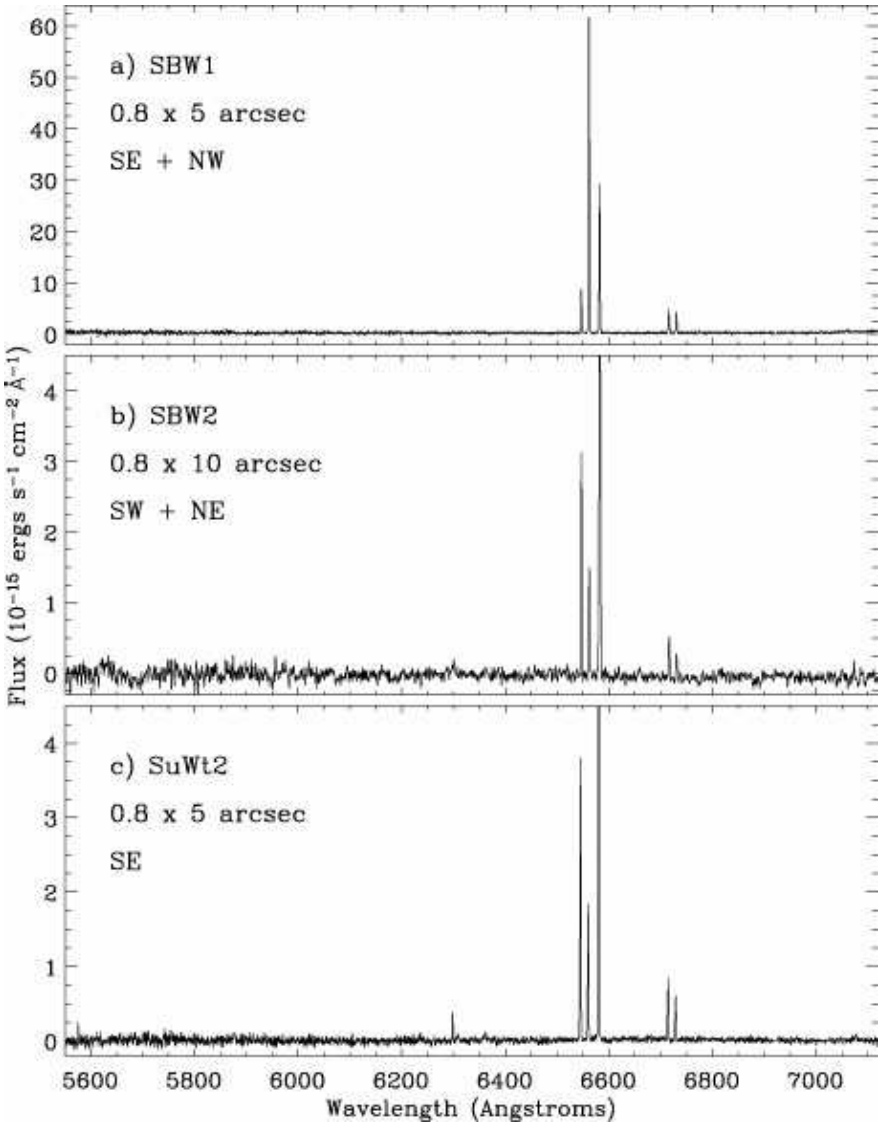

Fig. 7.— Extracted CTIO/4m RC Spec spectra of SBW1 (a), SBW2 (b), and SuWt2 (c). Aperture sizes and their approximate locations are noted in each panel.

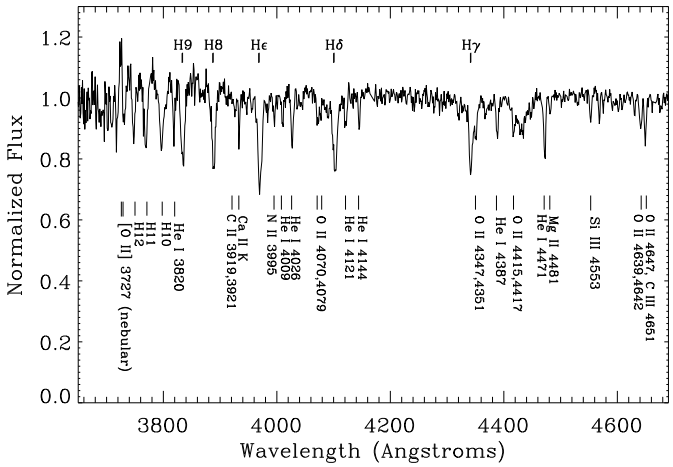

Fig. 8.— Blue spectrum of the central star of SBW1. The MK spectral type is approximately B1.5 Iab.

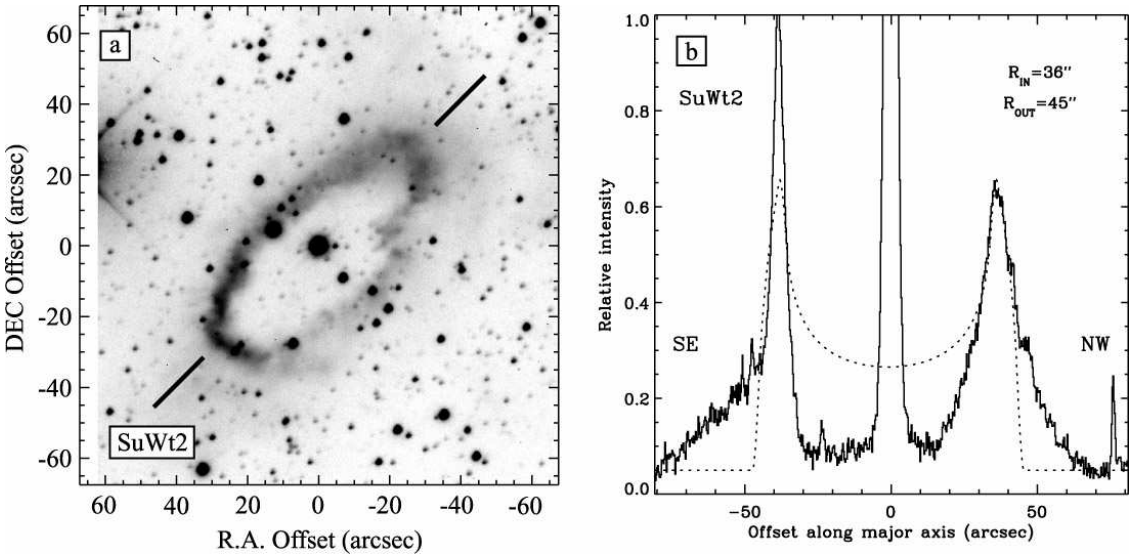

Fig. 9.— (a) Hα+[N II] image of SuWt2 obtained with the MOSAIC2 camera on the CTIO 4m telescope. (b) Same as in Figure 3, but for SuWt2. The intensity tracing cuts across the major axis of the ring (along P.A.=–45°). The diagonal lines in Panel *a* mark the orientation of the slit for the RC Spec observations, as well as the scan direction for Panel *b*. The central star is offset from the exact center of the ring by $\sim$1″ to the NW.

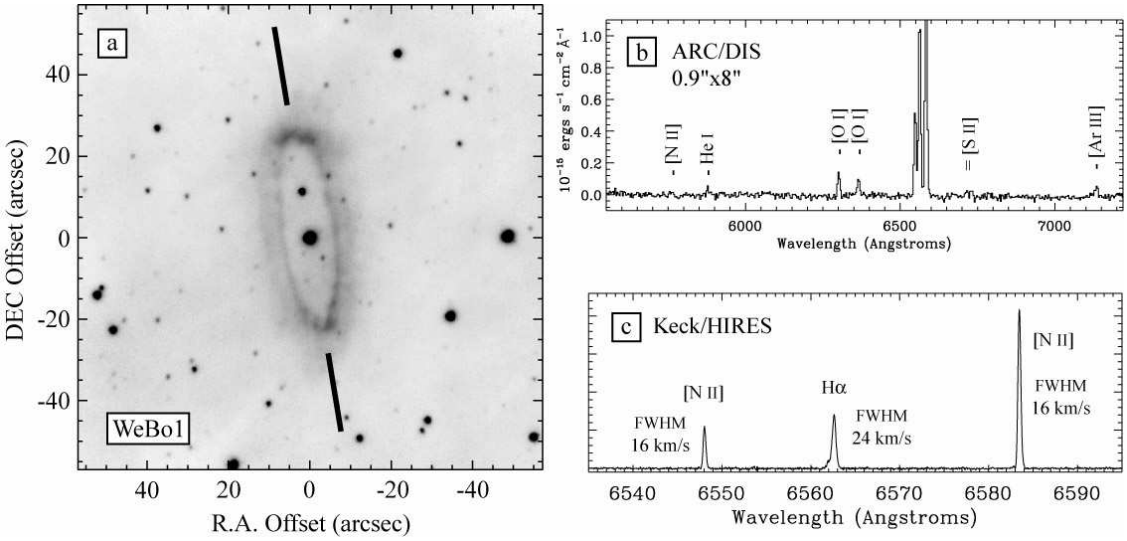

Fig. 10.— (a) Hα+[N II] image of WeBo1 obtained with SPICam on the ARC 3.5m telescope. (b) A low resolution red spectrum of WeBo1 obtained with DIS on the ARC telescope. (c) a higher resolution spectrum of the Hα+[N II] lines obtained with the HIRES spectrograph on Keck.